

Three-dimensional integral imaging of micro-objects

Ju-Seog Jang

Division of Electronics, Computers, and Telecommunications, Pukyong National University, 599-1 Daeyun-Dong, Nam-Gu, Pusan 608-737, Korea

Bahram Javidi

Department of Electrical and Computer Engineering, University of Connecticut, 371 Fairfield Road, U-1157, Storrs, Connecticut 06269-1157

Received November 24, 2003

We propose a method for displaying micro-objects in space that is based on three-dimensional (3D) integral imaging, in which elemental images are calculated from a two-dimensional sampling of the optical field along different depths by use of confocal scanning microscopy. Experimental results are presented to demonstrate that a uniformly magnified 3D biological specimen can be displayed in space, and thus integral imaging can be used for 3D display of confocal microscopy. To the best of our knowledge, this is the first report of 3D integral imaging of (semitransparent) micro-objects. © 2004 Optical Society of America

OCIS codes: 110.6880, 100.6890, 180.1790.

There has always been great interest in the visualization of micro-objects.¹ Integral imaging^{2,3} (II) has been studied for three-dimensional (3D) imaging, television, and visualization.⁴ To both record and display a 3D image of an object, lenslet elements with 1- or 2-mm apertures have been used.³ However, II cannot be applied to micro-objects smaller than each microlens. The use of magnifying lenses before the pickup process cannot be a solution, because magnification is nonuniform along the longitudinal depth direction, and thus the 3D shape cannot be preserved for a magnified image.⁵ Using a microlens array with lenslets much smaller than the micro-object is not a solution either, because diffraction in each microlens becomes significant, and thus the image resolution is degraded seriously.⁶

In this Letter we show that uniformly magnified 3D images of micro-objects can be displayed in space using II. To accomplish this, we use uniformly magnified two-dimensional (2D) sectioning images of a 3D micro-object along different depths that are obtained from confocal scanning microscopy. The ray information for 3D image formation is calculated from the sectioning images and used in II to display 3D micro-objects. Our approach can deal with semitransparent micro-objects, such as microbiological cells.

In the pickup (recording) process of II the direction and intensity information on the rays coming from a 3D object is spatially sampled by use of a lenslet (or pinhole lens) array and recorded by a 2D image sensor, as depicted in Fig. 1(a). The ray information sampled by each lenslet (or pinhole lens) is a demagnified 2D image with its own perspective, referred to as an elemental image. Reconstruction of a 3D image of the object from 2D elemental images is a reverse of the pickup process. The recorded 2D elemental images are displayed in a 2D display panel, such as a LCD panel, and then rays coming from the elemental images are redirected to form a real 3D image, as depicted in Fig. 1(b). In II, therefore, a true 3D image with full parallax

and continuous viewpoints can be produced optically in space.

II is well contrasted with commonly used stereoscopic techniques, which usually require supplementary glasses to evoke a 3D visual effect to observers.⁷ In stereoscopic techniques, however, observers see only a fixed viewpoint and may experience visual fatigue because of convergence–accommodation conflict.⁸

To obtain 3D images of micro-objects such as biological specimens, confocal (laser scanning) microscopy is widely used.¹ In this technique, sharply focused light is illuminated on a 3D specimen and reflected light (or fluorescent light, if the specimen is properly treated with dye) is detected. A 2D image of a slice of the specimen centered in the focal plane (called a sectioning image) is obtained by scanning the specimen at that focal plane. A stack of sectioning images (and thus a volumetric image) is obtained by sweeping through the specimen along the optical axis (i.e., depth) direction. To our knowledge, so far there has been no way to form a 3D image of a micro-object with a 2D display panel. The 3D nature of the volumetric image is visualized by use of a computer simulation, a sequential plane-by-plane display in the time domain, or a stereoscopic method that can produce visual fatigue.

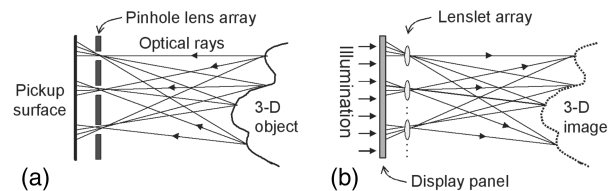


Fig. 1. Principle of 3D II. (a) Pickup process with a pinhole lens array. In the direct pickup process a lenslet array is used for high light efficiency. A pinhole lens array can be used when the pickup process is digitally synthesized to obtain elemental images according to ray optics. (b) Reconstruction of a 3D image with a lenslet array.

In our 3D display approach, II is used to form a true 3D image of a micro-object displayed in space. The image is a uniformly magnified version of the micro-object in both the lateral (x, y) and the longitudinal (z) scales. The elemental images are calculated from a volumetric image with sufficient resolution obtained from, for example, a confocal microscope. First, we assume that a sequence of images representing sections of the 3D micro-object are positioned either in front of or behind a hypothetical pickup pinhole lens array, as depicted in Figs. 2(a) and 2(b). Then, considering the sequence of sectioning images as a volumetric image

$$A_C(k) = \begin{cases} \exp(-\alpha k), & \text{if } \sum_{C=1}^3 \sum_{m=0}^{k-1} V_C(\beta_m x_i, \beta_m y_i, z_m) \neq 0 \text{ and } k > 1 \\ 1, & \text{otherwise} \end{cases}, \quad (2)$$

of the magnified micro-object, we synthesize elemental images by simulating the direct pickup process of an II system according to geometric optics. When the calculated elemental images are displayed with a lenslet array and a 2D display panel, observers view either a real 3D image or a virtual 3D image in the same way the sectioning images are positioned, as depicted in Figs. 2(c) and 2(d). The pitch (period) of the hypothetical pinhole array, denoted by p , should be equal to the pitch of the display lenslet array. Gap distance g should be properly selected for optimal focusing of the displayed 3D image for a given focal length of lenslets f . If the distance between the lenslet (or pinhole lens) array and the center sectioning image is L , g should be $Lf/(L+f)$ for virtual display and $Lf/(L-f)$ for real image display according to the Gauss lens law.

The light intensity distributions of sectioning images located at $z > 0$ should be mapped through corresponding pinholes into the pickup surface, and those at $z < 0$ should be mapped directly into the pickup surface.⁶ If the light intensity distribution of the k th sectioning image subtended by an angle of ψ for the i th pinhole is given by $V_C(x_i, y_i, z = z_k)$, where subscript $C = 1$ (for red), 2 (for green), and 3 (for blue), the light intensity distribution of the corresponding pickup surface $S_C(x_i, y_i, z = -g)$ becomes

$$S_C(x_i, y_i, -g) = \frac{1}{M(x_i, y_i)} \sum_{k=1}^N A_C(k) V_C(\beta_k x_i, \beta_k y_i, z_k), \quad (1)$$

where x_i and y_i are the local coordinates for the i th pinhole that positions at $x_i = y_i = 0$, and N is the number of sectioning images. $M(x_i, y_i)$ is a normalization factor, which is the number of times the pixel values are added at position (x_i, y_i) . $A_C(k)$ is introduced to take into account light absorption inside the semitransparent micro-object. Therefore backsectioning images suffer from more absorption than front sectioning images. The scaling factor β_k is given by $-z_k/g$, where the minus sign indicates inverted image mapping through the pinhole lens.

To avoid interference between the neighboring elemental images at the pickup surface, we set

$\psi = 2 \arctan(p/2g)$. The viewing angle of the 3D reconstructed images is also limited by ψ .⁹

To demonstrate our approach experimentally, we used 26 color sectioning images of a grape stamen tetrad, which is a four-cell product of meiosis in the male reproductive structure of a grape.¹⁰ The total depth and the lateral size of the micro-object are ~ 18 and $\sim 40 \mu\text{m}$, respectively. Each sectioning image was obtained from confocal microscopy and has a resolution of 512×512 pixels. A few samples are shown in Fig. 3(a). For simplicity we assume that there is uniform absorption inside the specimen:

where α is a positive number. $\alpha = 0$ implies a transparent object and $\alpha = \infty$ implies an opaque object. We synthesized the elemental images for virtual 3D image display. The elemental images for a low absorption coefficient (e.g., $\alpha = 0.05$) are illustrated in Fig. 3(b), where it is assumed that $z_1 = -17$ mm, $\Delta z = z_k - z_{k+1} = 0.9$ mm, and the size of each sectioning image equals 9.2 mm. Because there are 26 sectioning images, the 3D image depth of the displayed object is 22.5 mm. Thus the ratio of longitudinal to lateral magnification was ~ 5 in this experiment. In fact, we exaggerated the image depth to emphasize that a uniformly magnified image through the depth direction is displayed. The display lenslet array has 53×53 lenslets. Each lenslet is square shaped and has a uniform base size of $1.09 \text{ mm} \times 1.09 \text{ mm}$, with less than $7.6 \mu\text{m}$ separating the lenslets. The focal length of the lenslets is approximately 3 mm, and thus we set $g = 2.6$ mm. Thus the viewing angle ψ

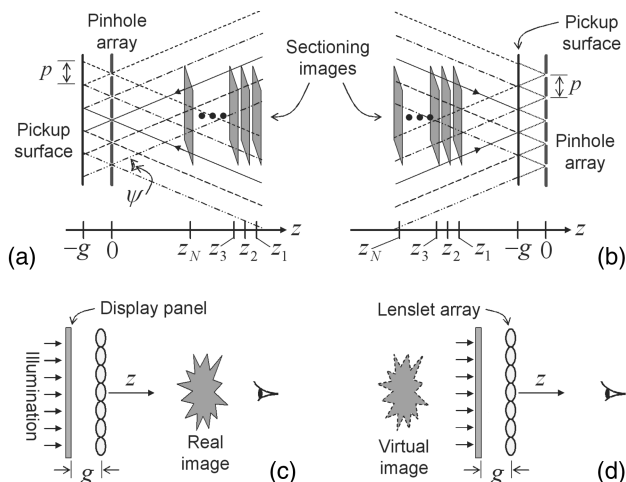


Fig. 2. Computer pickup for given sectioning images and optical 3D image reconstruction in space. The longitudinal position of the pinhole array is set at $z = 0$. Observers are assumed to be positioned at $z > 0$. (a) Pickup for real 3D image display. Locations of sectioning images along the z axis, z_1, z_2, \dots, z_N , are positive values. (b) Pickup for virtual 3D image display. Locations of sectioning images along the z axis, z_1, z_2, \dots, z_N , are negative values. (c) Real 3D image display. (d) Virtual 3D image display.

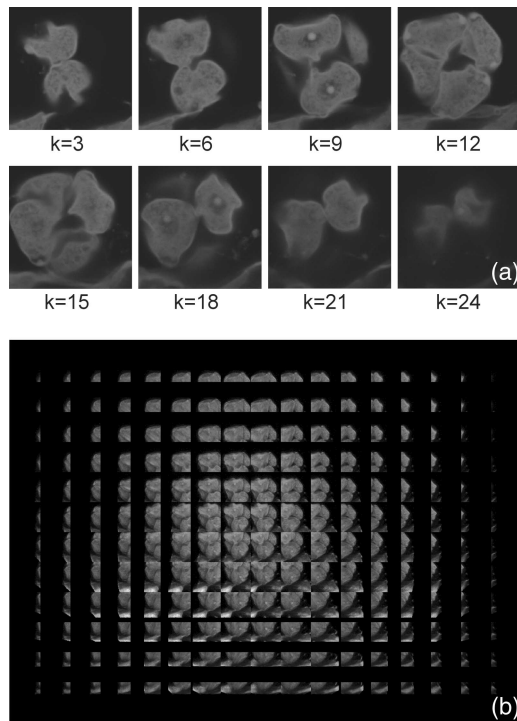


Fig. 3. Experimental results. (a) Sectioning images used in the experiments. (b) Synthesized elemental images.

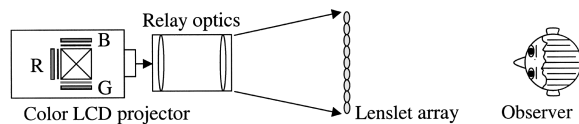


Fig. 4. Schematic diagram of an II projector used in the experiment.

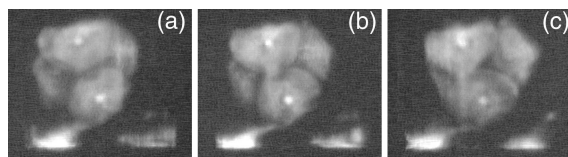


Fig. 5. Reconstructed 3D image displayed optically in space. As the viewing direction changes, the perspective varies continuously. (a) Left view. (b) Center view. (c) Right view.

is approximately 24° . For 3D image reconstruction as depicted in Fig. 2(d), we used an off-the-shelf LCD projector with three LCD panels as an integral imaging projector^{11,12} for 3D color image display, as shown in Fig. 4. Each panel has 1024×768 square pixels with a pixel pitch of $18 \mu\text{m}$. Each elemental image is represented by 60×60 pixels. Thus approximately 17×13 lenslets (or elemental images) were used to display the sectioning images. The optically reconstructed 3D image observed from three different directions are shown in Fig. 5. Each image was captured with a color CCD camera positioned at

$z \approx 20 \text{ cm}$. As the observation direction changes, the perspective of the 3D image displayed in space varies continuously, which demonstrates the 3D nature of the displayed image.

The resolution, view angle, and depth of focus of 3D integral images are limited.^{6,9,13} These limitations can be relaxed by use of high-resolution display panels and a time-multiplexing technique.^{9,12,14} There is a slight color mismatch between the elemental images shown in Fig. 3(b) and the reconstructed images shown in Fig. 5. This mismatch can be improved if we use a LCD projector and a CCD camera that can represent color more accurately. Application of our approach is not limited to microscopy. Sectioning images of other objects, for example, a volumetric image of the human body obtained from magnetic resonance imaging, can also be used to form and optically display a true 3D image in space.

In conclusion, we have presented a new 3D optical display method, in which sectioning images of confocal microscopy are used. Our experiment shows that uniformly magnified true 3D images of micro-objects can be optically displayed in space using II. Our method can assist physicians, biologists, scientists, and engineers in perceiving the 3D structure of micro-objects more vividly and accurately.

We thank Myungjin Cho (Pukyong National University) for his help with the experiments and Janey Youngblom (California State University) for allowing us to use the confocal microscopy images. This research was supported in part by the University Information Technology Research Center project of the Korea Ministry of Information and Communication. J.-S. Jang's e-mail address is jsjang@pknu.ac.kr; B. Javidi's is bahram@enr.uconn.edu.

References

1. J. W. Lichtman, *Sci. Am.* **271**, 30 (1994).
2. G. Lippmann, *C. R. Acad. Sci.* **146**, 446 (1908).
3. C. B. Burckhardt, *J. Opt. Soc. Am.* **58**, 71 (1968).
4. F. Okano, H. Hoshino, J. Arai, and I. Yuyama, *Appl. Opt.* **36**, 1598 (1997).
5. M. Born and E. Wolf, *Principles of Optics*, 6th ed. (Pergamon, Oxford, 1980), pp. 152–153.
6. J.-S. Jang, F. Jin, and B. Javidi, *Opt. Lett.* **28**, 1421 (2003).
7. T. Okoshi, *Proc. IEEE* **68**, 548 (1980).
8. T. Yamazaki, K. Kamiyo, and S. Fukuzumi, in *Proceedings of the International Display Research Conference* (Society for Information Display, San Jose, Calif., 1989), pp. 606–609.
9. J.-S. Jang and B. Javidi, *Appl. Opt.* **42**, 1996 (2003).
10. Animation available at <http://science.csustan.edu/confocal/Images/Animation/grapestamentetrad.htm>.
11. J.-S. Jang and B. Javidi, *Appl. Opt.* **41**, 4866 (2002).
12. J.-S. Jang, Y.-S. Oh, and B. Javidi, *Opt. Express* **12**, 557 (2004), <http://www.opticsexpress.org>.
13. H. Hoshino, F. Okano, H. Isono, and I. Yuyama, *J. Opt. Soc. Am. A* **15**, 2059 (1998).
14. J.-S. Jang and B. Javidi, *Opt. Lett.* **27**, 324 (2002).